Review article

Ora Bitton[a], Satyendra Nath Gupta[a] and Gilad Haran*

Quantum dot plasmonics: from weak to strong coupling

https://doi.org/10.1515/nanoph-2018-0218
Received December 13, 2018; revised February 2, 2019; accepted February 5, 2019

Abstract: The complementary optical properties of surface plasmon excitations of metal nanostructures and long-lived excitations of semiconductor quantum dots (QDs) make them excellent candidates for studies of optical coupling at the nanoscale level. Plasmonic devices confine light to nanometer-sized regions of space, which turns them into effective cavities for quantum emitters. QDs possess large oscillator strengths and high photostability, making them useful for studies down to the single-particle level. Depending on structure and energy scales, QD excitons and surface plasmons (SPs) can couple either weakly or strongly, resulting in different unique optical properties. While in the weak coupling regime plasmonic cavities (PCs) mostly enhance the radiative rate of an emitter, in the strong coupling regime the energy level of the two systems mix together, forming coupled matter-light states. The interaction of QD excitons with PCs has been widely investigated experimentally as well as theoretically, with an eye on potential applications ranging from sensing to quantum information technology. In this review we provide a comprehensive introduction to this exciting field of current research, and an overview of studies of QD-plasmon systems in the weak and strong coupling regimes.

Keywords: Plasmonic cavities; semiconductor nanocrystals; photoluminescence enhancement; Purcell effect; vacuum Rabi splitting.

1 Introduction

Plasmonics is a highly vibrant field of research at the boundary of optics and condensed matter physics. It provides a way to tune the properties of light by confining it to the regions below the diffraction limit [1]. The confinement of light at nanoscale dimensions is achieved through surface plasmon polaritons (SPPs), which are quasiparticles formed at the interface of a metal and a dielectric when light is coupled to the electron oscillations in the metal [1–3]. In extended structures (whose dimensions are larger than the wavelength of light) SPPs form propagating waves, but in finite-size nanostructures (nanospheres, disks, cones, etc.), the SPPs are localized in space and are therefore often called localized surface plasmons (LSPs). In SPPs or LSPs, the spatial variation of the charge density is much smaller than the wavelength of the light and hence they confine the light into regions far below the diffraction limit. This deep sub-wavelength confinement of light allows using plasmonic particles to operate as nanometric equivalents of antennas [4] or cavities [5], a realization that opened up a new frontier in the study of fundamental physics of light-matter interaction. In particular, the optical coupling of light to quantum emitters such as molecules and semiconductor nanocrystals quantum dots (QDs) has been tuned from the weak to the strong regime using plasmonic cavities (PCs). This has offered new opportunities for quantum control of light, application in quantum information processing and realizations of quantum devices such as single photon sources [6], transistors [7] and ultra-compact circuitry at the nanoscale. For fundamental studies of light-matter interaction, QDs carry an advantage over molecules due to their broad absorption spectrum, relatively narrow emission bands, and bright and stable photoluminescence (PL). Further, these properties of QDs can be tailored by changing their sizes and shapes.

It is therefore not surprising that an increasing number of experimental and theoretical studies has focused on composite QD-plasmon systems. In this review, we analyze these studies and provide some general context to understand their impact. The use of

[a]**Ora Bitton and Satyendra Nath Gupta:** These authors contributed equally to the review.
***Corresponding author: Gilad Haran,** Department of Chemical and Biological Physics, Weizmann Institute of Science, POB 26, Rehovot 7610001, Israel, e-mail: gilad.haran@weizmann.ac.il. https://orcid.org/0000-0003-1837-9779
Ora Bitton: Chemical Research Support, Weizmann Institute of Science, POB 26, Rehovot 7610001, Israel
Satyendra Nath Gupta: Department of Chemical and Biological Physics, Weizmann Institute of Science, POB 26, Rehovot 7610001, Israel

molecules as quantum emitters coupled with plasmons has been reviewed recently in a few articles, and we refer the interested reader to these references [8–12]. We start with a brief introduction to QD photophysics (Section 2), and then discuss the optical properties of the electromagnetic (EM) fields associated with PCs (Section 3). In Section 4 we discuss the underlying physics of composite QD-PC systems in which the QD is coupled to the PC and interacts with its confined EM fields. We describe in detail two coupling regimes, weak and strong coupling, each yielding different and unique optical properties. Sections 5 and 6 provide an overview of the wide range of research activities involving the study of composite QD-PC structures in these two regimes.

2 The photophysics of quantum dots

QDs, sometimes referred to as "artificial atoms", are very small semiconductor particles, only several nanometers in size. They are prepared in solution using colloidal chemistry and possess unique optical and electronic properties. The spectroscopic features of QDs involve transitions between discrete, three-dimensional (3D) particle-in-a-box states of both electrons and holes. This makes them very interesting and attractive solid-state quantum emitters.

To understand the photophysics of a QD, consider its interaction with light. When the QD absorbs a photon, an electron is excited from its valence band to the conduction band, creating a hole in the former. The electron-hole pair forms a new quasiparticle called an exciton, bound together by Coulomb interaction in a similar fashion to the hydrogen atom. In the simplest picture of the exciton in a bulk semiconductor, the electron and hole orbit each other at a distance (called the Bohr radius) that depends on the material. When the size of a semiconductor material is decreased below its "natural" Bohr radius, the electron and hole are effectively confined, making the exciton energy larger than in the bulk material and dependent on size [13, 14]. The ability to tune the spectroscopic features of QDs through their sizes has proven to be of huge importance for multiple applications [15–19].

A QD can be excited at essentially any energy larger than its band gap, which leads to a broad absorption band. The electron-hole pair is not a stationary state. Absorption is first followed by non-radiative electron relaxation to the lowest energy level in the valence band. A recombination of the electron and hole leads to spontaneous emission, which competes with nonradiative decay channels. Usually, the radiative lifetime is of the order of 10–50 ns and depends on size and material of the QD [20].

QDs are made from various semiconducting materials and exhibit optical emission at frequencies ranging from the ultraviolet to the near infrared region of the electromagnetic spectrum [19, 21–23]. Core-shell QDs exhibit unique optical properties that stem from their composition: a semiconductor material core, passivated by a coating, or a shell, also of a semiconductor material, but usually of a higher bandgap [24, 25]. This protects the QD from degradation of its optical properties resulting from aggregation and oxidation and leads to enhancement of the PL quantum yield of the core emission. Core-shell QDs can be up to 20 times brighter and 100 times more stable than organic dye molecules [26]. These QDs have also a relatively large dipole moment, corresponding to a strong oscillator strength. The typical dipole moment of fluorescent molecules is ~1D (Debye), while for QDs it can be 10 times larger.

Interestingly, QDs can sustain multiexcitonic states, such as a trion (a charged state consisting of an exciton plus an electron), a biexciton (BX) or even a triexciton (TX) involving Coulomb interaction between excitons [27, 28]. Some of these states are demonstrated in Figure 1A. In the emission process, multiple photons can be emitted through a cascade of emission from the BX or TX to the ground state via the single exciton state (SX). Some of the multiexciton energy levels are optically inactive ("dark"), while other are optically active ("bright") due to their spin orientations. Although the bright exciton is preferred for optical sensing and emission, dark excitons have received growing attention for their possible use in spin storage and as qubits [29].

The mentioned properties make QDs promising candidates for applications in nanophotonics and quantum optics [30]. They can serve as alternatives to organic dyes that are characterized by relatively fast photobleaching, low emission intensity and narrow absorption bands. However, despite their many advantages, QDs have two drawbacks that should be considered. Their large sizes compared to organic molecules limit the minimum size of optical cavities into which they can be inserted, and their intermittent on/off behavior ("blinking") can complicate ultrasensitive measurements.

3 Plasmonic cavities

Optical cavities confine light to a small volume. Placing an emitter, such as a QD, within this volume enables the

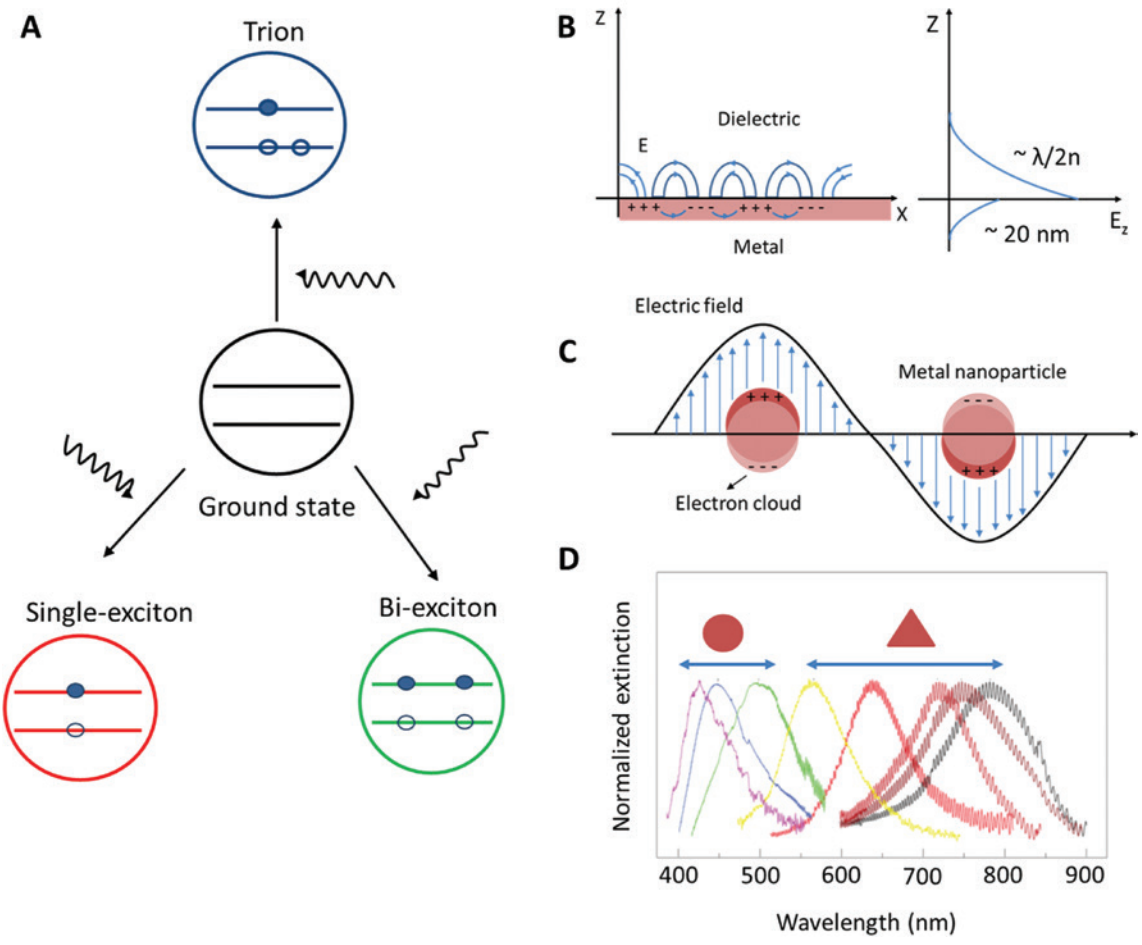

Figure 1: Excitations in QDs and plasmonic systems.
(A) Schematic representation of single-exciton and multi-exciton generation in QD. (B) Pictorial illustration of electromagnetic wave and surface charges at the metal-dielectric interface along with electric field decay with distance in a direction normal to the interface. (C) Schematic diagram of LSP on a metal nanoparticle. (D) Increasing the size of silver nanodisks and nanoprisms tunes their LSP spectra. As the size is increased, the plasmon peak shifts to higher wavelengths. (D) is reprinted with permission from Ref. 37.

study of light-matter interaction. Dielectric cavities made of mirrors, whispering gallery resonators, pillar structures or photonic crystals have been extensively used to study quantum optical phenomena [31, 32]. In this review we stress the corrolaries between such cavities and PCs, in which EM fields are confined to the vicinity of a metallic surface. In the current section, we will discuss the basic physics of PCs and their optical properties. Later, in Section 4, we will find that these properties can make PCs good alternatives to dielectric cavities for probing light-matter interaction.

As mentioned earlier, SPPs can be confined to transverse dimensions much smaller than possible with conventional optics. The electromagnetic field of a SPP at a dielectric-metal interface is obtained from the solution of Maxwell's equations in each medium combined with the associated boundary conditions. A classical result is that light in free space cannot be used for excitation of SPPs. Coupling of photons into SPPs can be achieved using a coupling medium such as a prism, a grating or a nanostructure to match the photon and SPP wave vectors [1, 33].

The field associated with an SPP is an evanescent wave that decays exponentially into the surrounding medium (Figure 1B). The decay length into a dielectric is ~ $\lambda/2n$ where n is the refractive index of the dielectric. The decay length into most metals of interest in the visible spectral range is significantly shorter, typically ~20 nm [34]. The lifetime of SPPs is on the sub-picosecond (ps) timescale. The exact decay rate strongly depends on the material and irradiation parameters. For instance, at the air-Ag interface, at 400 nm the plasmon decay time amounts to a few tens of femtoseconds (fs), while at 800 nm it is about 1 ps [35].

SPPs can be further geometrically confined to create LSPs. Excitation of LSP modes of a metal nanoparticle can only occur when the size of the particle is much smaller than the wavelength of the incident light. When light interacts with a metallic nanosphere, it drives the free electrons into oscillation at the same frequency of the field and induces a dipole moment inside the sphere (Figure 1C). The LSP spectral resonance and the shape of the extinction spectrum depend on nanoparticle composition, size and shape as well as on the local dielectric environment (Figure 1D) [36, 37]. At the resonance frequency, ω_c, the nanoparticle confines the electric field to its surface, with an amplitude that is much larger than that of the incident field, effectively turning the particle into a "cavity". Examples of calculated localized enhanced fields in plasmonic structures are shown in Figure 2A and B. The damping rate of the LSP, γ (i.e. the inverse of the LSP lifetime), determines the width of the resonance. It depends on the metal and the nanoparticle size and is typically within the range of 10^{13}–10^{14} Hz. There are several damping mechanisms for SPs and these have been discussed comprehensively in the literature [38–41]. The quality factor of an LSP resonance, Q, is defined as the ratio of the resonant frequency to the damping $\left(Q=\frac{\omega_c}{\gamma}\right)$ and determines the degree of losses in the PC and how efficiently it stores the plasmon energy. Due to their high losses, typical PCs have low quality factors (far below those of dielectric cavities). The strong amplitude of the confined LSP field has been found useful for various applications, such as: surface enhanced Raman scattering (SERS) [42, 43] surface enhanced spectroscopies [44] and photochemistry [45], in addition to the weak and strong coupling studies discussed below.

The lowest frequency LSP resonance of a metallic nanostructure is dipolar in nature. Beyond dipolar excitations, there exists a rich structure of higher-order LSP modes. However, these modes, which are characterized by higher frequencies, are usually optically inactive and therefore are difficult to detect and excite ("dark modes"). They can be observed by various near-field techniques [46–48].

When two metallic nanoparticles come close together to form a dimer, a gap is formed and the surface charge densities of the two nanoparticles interact very strongly [12, 49]. The dipolar SP modes of the two nanoparticles hybridize

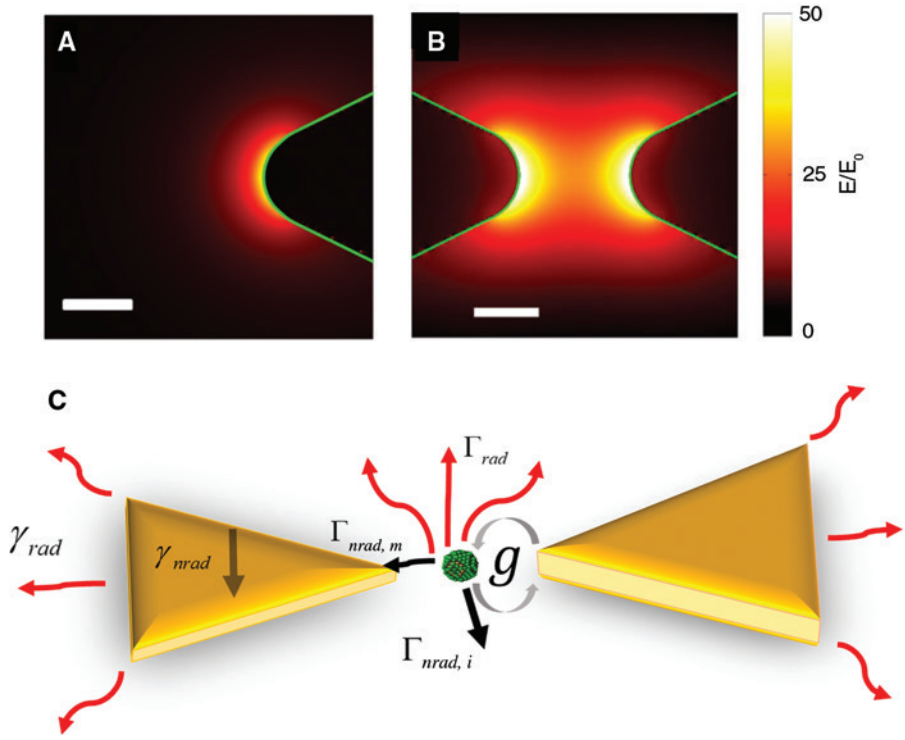

Figure 2: Interacting with a plasmonic cavity.
(A, B) Electromagnetic simulation of the electric field enhancement adjacent to a prism PC (A) and at the hotspot of a bowtie PC (B). The white bars represent 10 nm. (C) Schematic illustration of the various decay paths of a QD coupled to bowtie PC. The QD can emit either radiatively (Γ_{rad}) or non-radiatively through intrinsic processes $\Gamma_{nrad\text{-}i}$ or metal-induced damping ($\Gamma_{nrad\text{-}m}$). It can also transfer its energy to the plasmon mode which can emit light with a radiation rate γ_{rad} or be damped with a rate γ_{nrad}. Panels (A) and (B) are reprinted with permission from Ref. 139.

to form two distinct collective modes, known as the low-energy "bonding" mode and the higher-energy "antibonding" mode. Higher order multipoles can also contribute to this interaction and coupling between them leads to various hybridized states. The gap between the two nanoparticles, commonly termed a "hotspot", sustains a very large field enhancement. Specifically, when two prisms come close to form a bowtie, a dramatic field enhancement is obtained in the gap that can reach ~100-fold (Figure 2A, B). In fact, the junction between any arrangement of nanoparticles such as dimers, trimers or higher-order aggregates, can give rise to highly intense and localized fields. This property of "hotspots" is exploited in SERS, where the chemical signature of a single molecule can be observed. This electromagnetic focusing effect in a strongly coupled plasmonic system makes the "hotspot" a desired cavity suitable for the study of light-matter interaction.

4 The exciton-plasmon composite system: background

In this section we will overview the underlying physics of a composite system comprising an emitter embedded in or near a plasmonic structure.

Consider an emitter, characterized as a two level system with a ground state $|g>$ and an excited state $|e>$, a transition frequency ω_{eg}, a transition dipole moment $\vec{\mu}_{eg}$ (which translates into an oscillator strength f) and a spontaneous emission rate Γ. The emitter is placed inside a cavity characterized by resonance frequency ω_c and a damping rate γ, corresponding to a quality factor Q already introduced. The strength of the coupling between the emitter and the cavity, g, is related to the rate of energy transfer between the two and can be written as follows:

$$g = \vec{\mu}_{eg} \cdot E = \vec{\mu}_{eg} \cdot \sqrt{\frac{\hbar\omega_c}{2\epsilon_0\epsilon_r V_{\text{eff}}}}. \quad (1)$$

Here, E is the electric field within the cavity, ϵ_0 is the permittivity of vacuum and ϵ_r is the relative permittivity. V_{eff} is the effective mode volume of the electric field and encodes the spatial extent of the localized density of states (LDOS). Smaller mode volumes lead to larger LDOS values and stronger cavity-emitter coupling strengths. When N emitters are introduced in the cavity, the coupling strength becomes $\sqrt{N}$ larger [50].

In the weak coupling regime, the eigenstates of the coupled system are the same as those of the uncoupled system, but the PL of the QD may change significantly through the well-known Purcell effect (Section 5). In the strong coupling regime, the interaction is strong enough so that not only the spontaneous emission rate is modified but also are the energy levels of the system. The excited quantum emitters and the electromagnetic modes in the cavity reversibly and coherently exchange energy with a fast exchange rate g before any loss occurs. The energy levels of the hybrid system are very different from those of the quantum emitter and the electric field separately. This leads to a splitting in the cavity spectral response, known as Rabi splitting (see Section 6).

The transfer from weak to strong coupling can be achieved either by increasing the coupling strength g or by decreasing the decay rates of the cavity and the emitter. g can be increased by enhancing the oscillator strength of the emitter, enhancing the electric field in the cavity, or decreasing the effective mode volume. The emission rate Γ depends on the identity of the emitter and can often be reduced at low temperatures. The cavity decay rate γ can be decreased by reducing cavity losses, i.e. increasing the cavity Q. For achieving strong coupling with a single QD, a very low mode volume or very small losses are required. An ensemble of QDs generates a larger effective dipole moment, making it easier to achieve the strong coupling regime as has been demonstrated in a few experiments to be discussed in Section 6.

Dielectric cavities are characterized by relatively large mode volumes (0.1 μm^3), limited by the wavelength of light. However, in order to achieve strong coupling, they can be constructed with extremely high Qs (~10^4), which requires pumping them with light sources of ultra-narrow linewidth and operating at cryogenic temperatures. PCs have rather modest Qs, of the order of ~10–20, but their mode volumes can be much smaller than the diffraction limit. They can therefore reach the strong coupling limit even at room temperature and using light sources of modest linewidth.

In the following sections, we will discuss in greater detail the physical mechanisms operative in each coupling regime, while focusing on theoretical and experimental results achieved with QD-PC systems.

5 The weak coupling regime

5.1 Underlying physics

When an emitter is weakly coupled to a PC, its PL is modified in multiple ways [51–54], which may include reshaping of its spectrum and polarization, intensity enhancement or quenching, modulation of radiative and non-radiative

decay rates, changes in blinking behavior and more. In this regime, the wave functions of the plasmons and excitons are unperturbed by the interaction. Plasmon-enhanced fluorescence was first explored in conjunction with studies of surface-enhanced Raman spectroscopy in the 1970s and 1980s [55]. Already at that time, semiclassical models were developed to describe surface-enhanced fluorescence (SEF) based on the electromagnetic coupling of dipole emitters with plasmon modes [56, 57]. In recent years, the interest in studying SEF has significantly grown, as has the ability to judiciously control various aspects of the phenomenon.

One of the most well-known effects studied in the weak coupling regime is the modification of the spontaneous emission rate of an emitter, which was computed by Purcell in the case of a single-mode cavity [58]. He attributed the enhancement of the spontaneous emission of a quantum emitter within a cavity to the increased local density of states compared to free space. As the emission rate of a quantum emitter is linearly proportional to the LDOS, the presence of a cavity directly enhances it. The Purcell factor, F_p, is defined as the ratio of the spontaneous emission rate in a cavity, Γ_c, to the emission rate in free space, Γ_0:

$$F_P = \frac{\Gamma_c}{\Gamma_0} = \frac{6\pi c^3}{n^3 \omega_c^3} \frac{Q}{V_{\text{eff}}} \tag{2}$$

Here, n is the refractive index within the cavity and c is the speed of light. The Purcell factor is readily seen to be proportional to the square of the coupling strength, g (compare equation 1). As noted in the previous section, although dielectric cavities are characterized by high Q values, their mode volumes are relatively large, making it challenging to obtain large Purcell factors. Experimental values of the Purcell factor in dielectric optical cavities are presently limited to ~75 [31, 59]. PCs, on the other hand, support strong field enhancements and a strongly modified LDOS, thus providing a flexible means for controlling the spontaneous emission rate of quantum emitters. Importantly, PCs open several decay routes for an emitter, and the Purcell factor is defined through the relative increase in the *overall* decay rate.

When an emitter is positioned adjacent to or within a PC under weak-coupling conditions, both excitation rate and emission rate are modified. First, the enhanced local field couples to the emitter and increases its excitation rate Γ_{exc}. For this enhancement, overlap of the absorption spectrum of the emitter with the LSP band is required. The excitation enhancement is strongly dependent on the emitter dipole orientation relative to the electric field polarization direction of the PC. In the subsequent emission process, the presence of the PC alters the direct radiation channel of the emitter, which also requires spectral overlap of the emission and LSP spectra. The excited-state energy of the emitter can also be transferred to the metal in a process akin to Förster resonance energy transfer [60]. The energy is eventually dissipated in the metal (ohmic loss), though it can be emitted by the metal with a very low quantum efficiency. Coupling between dipole emitters and SPs may also modify the emission direction and polarization [51–54]. The light emission from a quantum emitter can be steered in a specific direction in space by either using simple anisotropic plasmonic nanostructures that exhibit angular and polarization dependent SP resonances or by designing more complex, multicomponent plasmonic nanostructures, such as optical Yagi-Uda nanoantennas [61, 62]. This change in angular emission usually originates from energy transfer from the emitter to the resonant SP mode of the optical antenna with a specific emission angle distribution. The modification in the angular emission might affect the collection efficiency or in other words, the fraction of light collected by the microscope objective, especially for a low numerical aperture objective. Therefore, in order to quantitatively interpret PL intensity measurements, one needs to study the radiation pattern and collection efficiency.

A scheme indicating the various recombination channels of a QD near a plasmonic particle is shown in Figure 2C. Whether an overall enhancement or quenching is observed in the PL measurement of a given system is determined by the relative contribution of each of the above channels. Modification of the spontaneous emission rate, Γ_c, which directly determines the Purcell factor, involves both changes in the radiative decay and the non-radiative decay. Consequently, extracting separate excitation and decay rates from time-dependent PL measurements is not straightforward. Semiconductor QDs enable more readily the separation of excitation and emission effects compared to organic molecules. Their absorption spectrum extends over a broad range, and it is simple to overlap it with the spectrum of plasmonic particles of various sizes and material systems. The emission spectrum, on the other hand, is narrow and well separated from the absorption.

Experimental efforts to measure the various photophysical processes involved in QD-PC interactions in the weak coupling regime are described next.

5.2 Plasmonic nanostructures and QDs: observing interactions

Studies of QD-PC composite systems in the weak coupling regime are numerous. Control of the emission of an

ensemble of QDs was achieved by coupling them to various metallic structures, such as films [63–65], nanostructured films [66–68], plasmonic antenna structures [69–76], plasmonic rings [77], metamaterials [78], nanoslits [79] and more. As mentioned earlier, several aspects play an important role in determininig the measured photoluminscence, and these are the excitation and emission rates, as well as the radiation pattern.

Some authors designed their experiment to measure excitation enhancement only and showed a moderate several-fold PL enhancement [63, 69]. However, the majority of published works aimed to achieve greater enhancement by overlapping QD emission with LSP spectra and therefore increasing the emission, or even a combination of excitation and emission. For instance, Song et al. [66] studied CdSe/ZnS QDs in contact with a periodic array of silver nanoparticles. They observed a spontaneous emission rate enhancement of 10 that, due to competition with nonradiative emission channels of the QD, led to an enhancement of the fluorescence intensity by up to ~50 folds. Brolo et al. [67] showed that the coupling of QDs to the SP modes of nanohole arrays created in a metal film that can yield an even larger PL enhancement of two orders of magnitude. As the PL decay rate manifested a Purcell factor of ~70 only, the authors suggested that enhancement of the excitation was also involved. Wang et al. [70] studied the time-resolved PL decay dynamics of QDs on an Au disk array. They showed that the coupled QD-SP system scatters strongly into a direction that is commensurate with the direction and polarization of the SP excitations. Hence, when the detection angle was aligned to this direction, the PL decay rate was accelerated. Belacel et al. [73] demonstrated experimentally the control of the radiation pattern of QDs deterministically positioned on a gold patch antenna. For certain locations within the antenna the emitters were shown to radiate in a highly directional pattern. They obtained Purcell factors ranging from 70 to 80. Ultra-strong Purcell factors were achieved by Hoang et al. [75] who studied a hybrid structure of a single silver nanocube separated by a thin polymer spacer layer containing QDs from a gold film. They showed a Purcell factor of 880 and simultaneously a 2300-fold enhancement in the total fluorescence intensity (Figure 3A). These enhancement values are the largest achieved so far with QDs. They were explained by the unique properties of the nanocube configuration; it maintains a large field enhancement of up to 200 folds and yields low non-radiative losses [82]. The nanocube exhibits also a highly directional radiation pattern, leading to a significant increase of the collection efficiency. This increase in collection efficiency is one of the factors that leads to such high measured fluorescence enhancements.

A similar configuration has been used earlier by the same authors to explore the Purcell enhancement with dye molecules [83]. When the emitters were resonant with the plasmon mode, the nanocube yielded a dramatic Purcell factor of 1000 with a spacer thickness of 8 nm and even 2000 with a thickness of 5 nm. Multiple investigations with dye molecules demonstrated ~1000-fold fluorescence intensity and radiative rate enhancements [84–89]. Although these values have rarely been reached with QDs, these emitters possess several advantages over molecules, as mentioned already, including their higher photostability and larger oscillator strength, which facilitates attaining the single particle level.

Indeed, ever since the emergence of this field there were multiple attempts to control and study the PL of individual QDs, rather than an ensemble of particles [80, 90–104]. Early on, Shimizu et al. [90] studied the fluorescence behavior of single CdSe(ZnS) core-shell QDs interacting with a rough metal film. They found a significant reduction in the single QD exciton lifetimes (by a factor of ~1000), which enabled them to observe emission from both neutral and charged excitons and a complete conversion of the QD emission polarization to linear. Ratchford et al. [80] used atomic force microscopy (AFM) nanomanipulation to controllably position a single Au NP near a CdSe/ZnS QD (Figure 3B). They showed that the PL enhancement is moderate below a distance of 20 nm due to a significant contribution of nonradiative processes. They calculated a Purcell factor of up to 145 but a radiative decay rate enhancement of only ~8. Urena et al. [95] demonstrated a moderate PL enhancement as well, but showed that the antenna mode fully determines the radiation pattern of a single QD. When a QD is coupled to a dimer gap antenna, the radiation pattern changes dramatically and transforms to that of a linear dipole horizontally aligned along the antenna axis. This serves as evidence for the coupling between the QD and the antenna. Yuan et al. [97] used a similar configuration to that of Hoang et al. [75], mentioned earlier, but studied a single QD. They showed that when the QD emission is coupled to a plasmonic gap mode, the radiative decay channels dominate and large Purcell factors of two orders of magnitude can be achieved. They also found that the BX emission quantum yields can be enhanced to a level which is comparable to the single excitons. Similar results were obtained by Matsuzaki et al. [104], who controllably positioned an individual QD in the near field of gold nanocone antennas and enhanced the radiative decay rates of both monoexcitons and biexcitons by ~100 folds. Their finding that the monoexciton and biexciton emission rates are enhanced by about the same factor implied

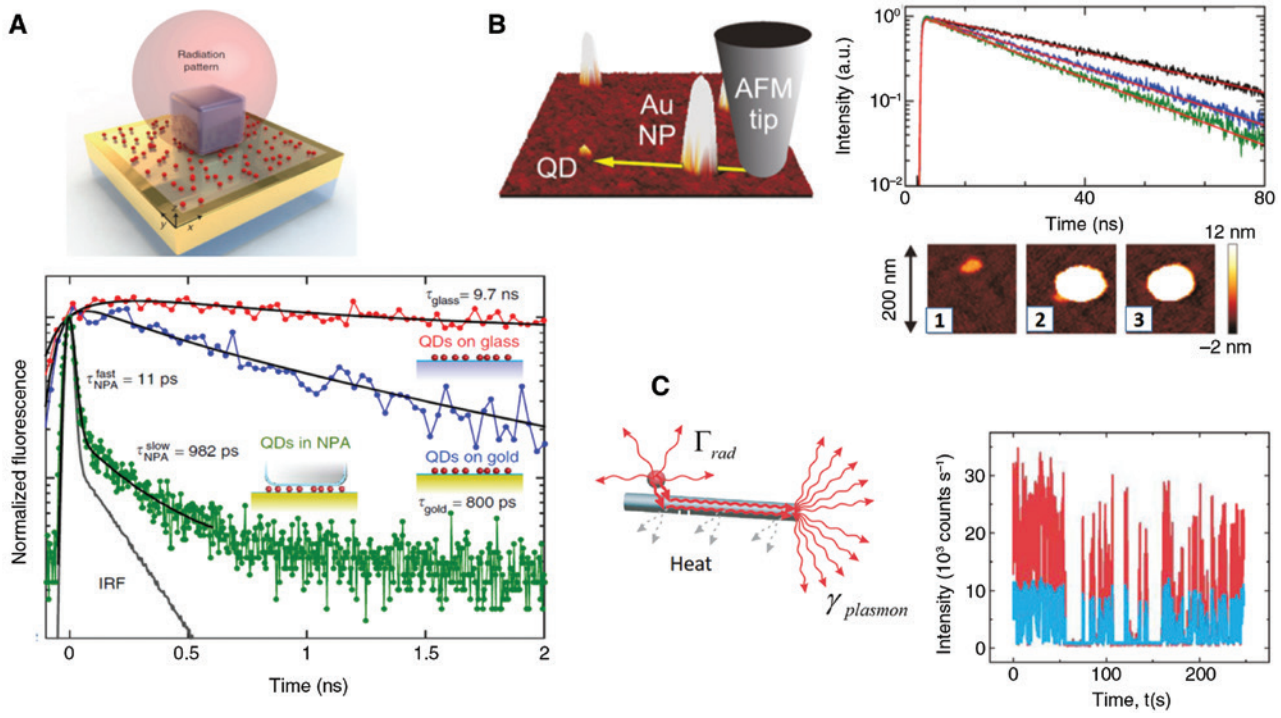

Figure 3: Probing and employing weak coupling.
(A) Top: 3D illustration of a single silver nanocube separated from a gold film by a thin polymer spacer layer containing QDs. Bottom: Normalized time-resolved fluorescence of QDs on a glass slide (red) compared with QDs on an Au film (blue) and coupled to a single naoncube as in the top panel (green). The instrument response function (IRF) is also shown. Fits to exponential functions convolved with the IRF are shown in black. Panel (A) is reprinted from Hoang et al. [75] (B) Left: AFM image of a QD and Au NPs. The yellow arrow denotes the path of the Au NP as it is being pushed by the AFM tip. Right: Gradual change in the QD PL lifetime due to the approaching Au NP. PL lifetimes of 35 ns (black), 26 ns (blue), and 22 ns (green) correspond to AFM images (1), (2), and (3), respectively. (B) is reprinted with permission from Ratchford et al. [80] Copyright 2011 American Chemical Society (C) Left: Illustration of a QD coupled to a nanowire. The QD can emit either into free space or into the guided SPs of the nanowire. Right panel: Time trace of fluorescence counts from the QD (red) and scattered light from the end of the coupled nanowire (blue). QD blinking leads to correlated fluctuations in the two signals. Panel (C) is reprinted by permission from Springer Nature, Akimov et al. [81], copyright 2007.

that their dipole orientations were similar to each other. To verify this hypothesis, they showed that the angular radiation patterns for the monoexciton and biexciton are similar. Takata et al. [103] also observed the involvement of higher excitonic states of a QD when they approached it with a silver-coated AFM tip. They recorded conversion from single-photon to multiphoton emission with a reduction of the emission lifetime as the QD-Tip distance decreased. The increased probability of emission from the BX state, a unique feature of QDs, was explained by quenching of the SX state due to resonance energy transfer to the tip.

5.3 Plasmonic nanostructures and QDs: towards potential applications

Recently, QD-PC composite systems in the weak coupling regime have been used to demonstrate unique features that can be very useful for faster, more compact optical devices. Here, we will mention a few of these results.

SPP generation by individual emitters coupled to a metallic nanowire received much interest [81, 98, 105, 106]. The ability to create and control individual quanta of plasmonic excitations accompanied by guided radiation with subwavelength localization can pave the way to new optoelectronic devices, such as single-photon sources and transistors. In a pioneering work, Akimov et al. [81] showed that when a single CdSe QD is optically excited in close proximity to a silver nanowire, emission from the QD couples directly to guided SPs in the nanowire and generates single, quantized plasmons (Figure 3C). Li et al. [106] showed more recently that the quantum yield of SP formation for a single QD coupled to a nanowire can be optimized by varying the distance of the QD from the surface, reaching an impressive maximal yield of 21%. The angular radiation pattern of the QD changed significantly when coupled to the nanowire, showing a nearly symmetric

pattern with respect to the nanowire axis. Similar nanowire configurations have also been used with molecules in order to perform SERS at a junction located remotely from the site of laser illumination [107–109].

Curto et al. [62] demonstrated unidirectional emission by coupling a single QD to a more complex structure, a plasmonic Yagi-Uda antenna. Indeed, they found that the PL from their devices was strongly polarized and highly directed into a narrow forward angular cone. Unidirectional emission (which was also demonstrated with organic dyes [110–112]) can provide a route to effectively communicate light to, from, and between nano-emitters.

Finally, Tang et al. [113] developed a plasmon-QD hybrid nanosystem with addressable emitters. They demonstrated selective far-field excitation and detection of two QDs coupled to a U-shaped gold nanostructure. The gold nanostructure functioned as a nanocavity to enhance emitter interactions and a nanoantenna to make the emitters selectively excitable and detectable. The authors were able to obtain emission from either QD interchangeably, with a Purcell factor of up to ~130 for each emitter.

6 The strong coupling regime

Significant advances in nanofabrication techniques have facilitated controlling parameters like spatial geometry and building block composition of hybrid systems combining emitters with plasmonic cavities. Thus, for example, it has become possible to reduce significantly the mode volumes of PCs, so as to achieve the strong coupling regime. Strong coupling between individual self-assembled QDs and dielectric cavities such as a photonic crystal-slab nanocavity [114], a micropillar [115] or a microdisk [116] had been successfully demonstrated already some years ago. However, these experiments required cooling the system to liquid helium temperatures. Achieving strong coupling between an emitter and cavity at room temperature and with modest light sources is desirable for developing robust applications in quantum information technology. One approach is to use an ensemble of emitters in order to increase the coupling enough to reach the strong coupling regime under ambient conditions, as has been shown in a number of studies (e.g. [117–120]). As discussed in Section 2, PCs offer an alternative to these systems for realizing strong coupling at room temperature. Indeed, in recent years strong coupling has been explored with PCs using both ensembles of molecules and individual molecules [121–126]. The endeavor to achieve strong coupling between the excitons of QDs and PCs, which is also gaining momentum rapidly, is the topic of this section of the review.

Theoretical investigations have delineated the conditions for realizing the strong coupling regime with QDs using different geometries of metal nanostructures. In an early contribution, Chang et al. [127] theoretically described a method for achieving strong coupling between individual emitters (QDs) and the SPPs of a conducting nanowire or a metallic nanotip at optical frequencies. They showed that it is possible to direct the optical emission almost entirely into the plasmon modes. Later, Truegler and Hohenester [128] showed using the boundary-element method that the strong coupling regime can also be observed between a single quantum emitter, such as a molecule or colloidal quantum dot, and a metal nanoparticle, which should be detected in the fluorescence spectrum via splitting of the emission peak. More recently, it was predicted by Savasta et al. [129], using scattering calculations, that strong coupling can be achieved by placing a QD in a cavity formed by two metallic nanoparticles. These theoretical studies (and others [130–132]) forecasted the unprecedented observation of strong coupling with individual QD emitters at room temperature. Before moving to the various experimental realizations of these predictions, let us dwell a bit more on the minimal model required to understand the interaction between an emitter and a cavity in the strong coupling regime.

6.1 Underlying physics

When quantum emitters are strongly coupled to an optical cavity, the wave functions of the emitters and cavity mix together. A simple model to describe strong coupling takes into account two coupled harmonic oscillators, whose properties are then obtained using either a classical, a semiclassical, or a quantum approach [133]. The full quantum mechanical approach usually starts with the Jaynes-Cummings (JC) Hamiltonian [134]. In the case of a single two-level QD interacting with a cavity mode in the limit of negligible dissipation, this Hamiltonian is written as follows:

$$H = \hbar\omega_c a^\dagger a + \frac{1}{2}\hbar\omega_{eg}\sigma_z + \hbar g(a\sigma_+ + a^\dagger\sigma_-) \tag{3}$$

Here, $a^\dagger$ and a are the field creation and annihilation operators, respectively, of the cavity mode with energy ω_c. σ_z, σ_+ and σ_- are Pauli matrices that represent the energies of the ground and excited states and generate transitions

between them, respectively. At resonance, the eigenstates and eigenvalues of the JC Hamiltonian are given by

$$|\pm\rangle_n = \frac{1}{\sqrt{2}}(\pm|e, n_{ph}\rangle + |g, n_{ph}+1\rangle) \tag{4}$$

$$E_{\pm} = \hbar\omega_c\left(n+\frac{1}{2}\right) + \hbar g(n_{ph}+1) \tag{5}$$

where n_{ph} is the number of photons in the cavity, $|g, n_{ph}+1\rangle$ is a state with the emitter in the ground state and $n_{ph}+1$ photons in the cavity, while $|e, n_{ph}\rangle$ is a state with the emitter in the excited state and n_{ph} photons in the cavity. Now the energy difference between the two levels can be written as

$$\Omega_R = 2\hbar g(n_{ph}+1) = 2\hbar\tilde{\mu}_{eg}\sqrt{\frac{\hbar\omega}{2\epsilon_0 V_{\text{eff}}}}(n_{ph}+1) \tag{6}$$

Thus, in order to increase the coupling strength so as to overcome the dissipative broadening of both cavity (γ) and emitter (Γ), the cavity mode volume (V_{eff}) should be made smaller and the emitter should be of large oscillator strength f. Another important fact to note from equation (6) is that the two energy levels split even in the absence of any photon. This phenomenon is called vacuum Rabi splitting: the vacuum state of the electromagnetic field couples with the electronic transition of the emitter. In case of multiple (N) emitters, the Rabi splitting scales with $\sqrt{N}$ [50]. A schematic illustration of Rabi splitting is shown in Figure 4A.

In fact, the electronic structure of N two-level systems coupled to a PC is a bit more complex. Overall, $N+1$ collective states are generated, out of which only two (termed P_+ and P_-) are bright, while the remaining N-1 are collective dark states. Thus, the wavefunction of the hybrid state can be delocalized over N QDs within the mode volume, leading to the possibility of modifying electronic and energy transport of the QDs. Another characteristic of the coupled QD-plasmon systems is the dispersive nature of the photonic component. Anticrossing is observed in dispersion curves at the intersection of the nondispersive emitter band and the dispersive optical component (Figure 4B). The Rabi splitting is defined as the minimum energy gap between the anitcrossing curves. The lifetimes of the P_+ and P_- states depend on the relaxation times of the plasmon and emitter modes. As the photon lifetime in a plasmonic cavity is very short (~50 fs), it is expected that the lifetime of the hybrid states will not be much longer. (But see Wang et al. [135] for a different result.)

6.2 Experimental realization

We start our discussion of experiments observing strong coupling in QD-PC systems with studies involving an ensemble of QDs. Gomez et al. [136–138] demonstrated

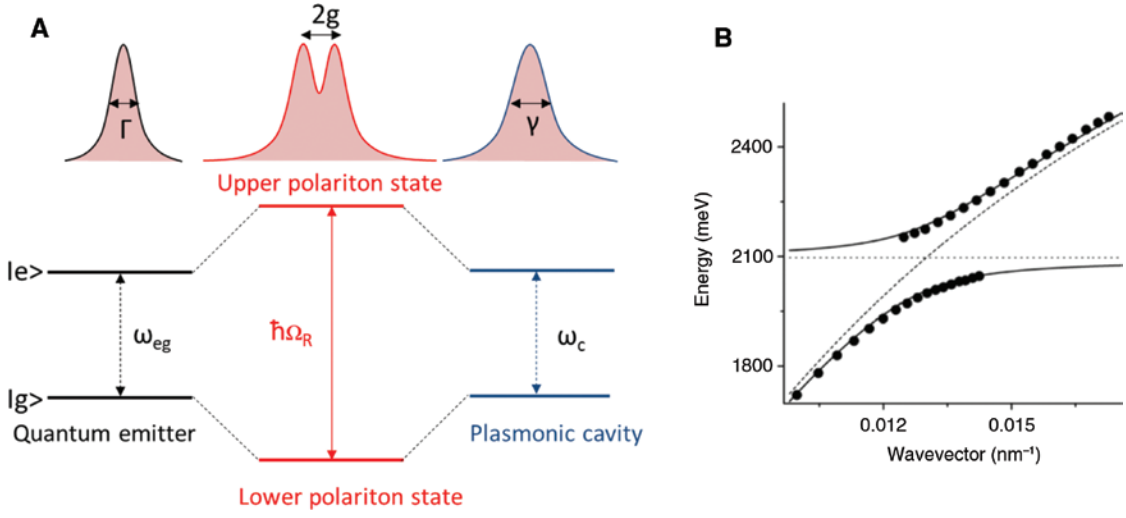

Figure 4: Principles of strong coupling.
(A) Schematic of resonance interaction between a two-level QD and a confined electromagnetic field in a PC, which results in two new hybrid states separated by Rabi splitting ($\hbar\Omega_R = 2g$). Upper panel: manifestation of strong coupling between QDs and a PC in the experimentally observable spectrum, splitting of the spectrum. (B) Anti-crossing behavior of a strongly coupled system consisting of a silver film and a concentrated cyanine dye in a polymer matrix. The data points are the dip energies in reflectance spectra as a function of the wave vector. The dashed and dotted lines represent the dispersion relation of the uncoupled surface plasmon and the exciton energy of the cyanine dye. The full lines are the calculated polariton energies. Panel (C) is reprinted with permission from Bellessa et al. [126].

strong coupling between a film of QDs and an SPP mode using angle-dependent reflectivity measurements in the Kretschmann-Raether configuration at room temperature. In their initial work [136], the QDs were spin-coated onto a thermally evaporated silver film on a cover slip, which was then attached to a right-angle glass prism using an index matching oil. P-polarized white light was coupled at a range of angles of incidence to tune the plasmon excitations in and out of resonance with the excitons of the QDs and demonstrate QD-plasmon interaction. The observed dispersion curve was fitted using the coupled oscillator model, and a Rabi splitting of 112 meV was extracted. In subsequent works, they also investigated the dynamic aspects of this interaction along with the effect of tuning the QD sizes [137, 138]. In another experiment involving an ensemble of emitters, Wang et al. [135] investigated the dynamics of strong coupling between CdSe QDs and the plasmons of a subwavelength gold nanohole array using steady-state spectroscopic methods as well as transient absorption measurements. In this work, holes were drilled in a 200 nm thick gold film using a focused ion beam. This was then followed by drop casting CdSe QDs onto the nanohole array. A large Rabi splitting of 220 meV was demonstrated. The lifetime of the QDs in the strong coupling regime was found to be only slightly shorter than the lifetime of bare CdSe QDs. As already noted, the lifetime of the dressed state is governed by fast decay mechanism, i.e. the damping time of the plasmon mode, which is of the order of fs. This expectation was not obeyed here, and this anomaly was attributed to a phonon bottleneck effect but requires further investigation.

Santhosh et al. [139] made the first attempt to realize strong coupling with individual QDs. They lithographically fabricated silver bowtie cavities and integrated them with QDs to observe vacuum Rabi splitting at room temperature. The maximum Rabi splitting achieved for a single QD was 176 meV (Figure 5A). For the case with two QDs, the

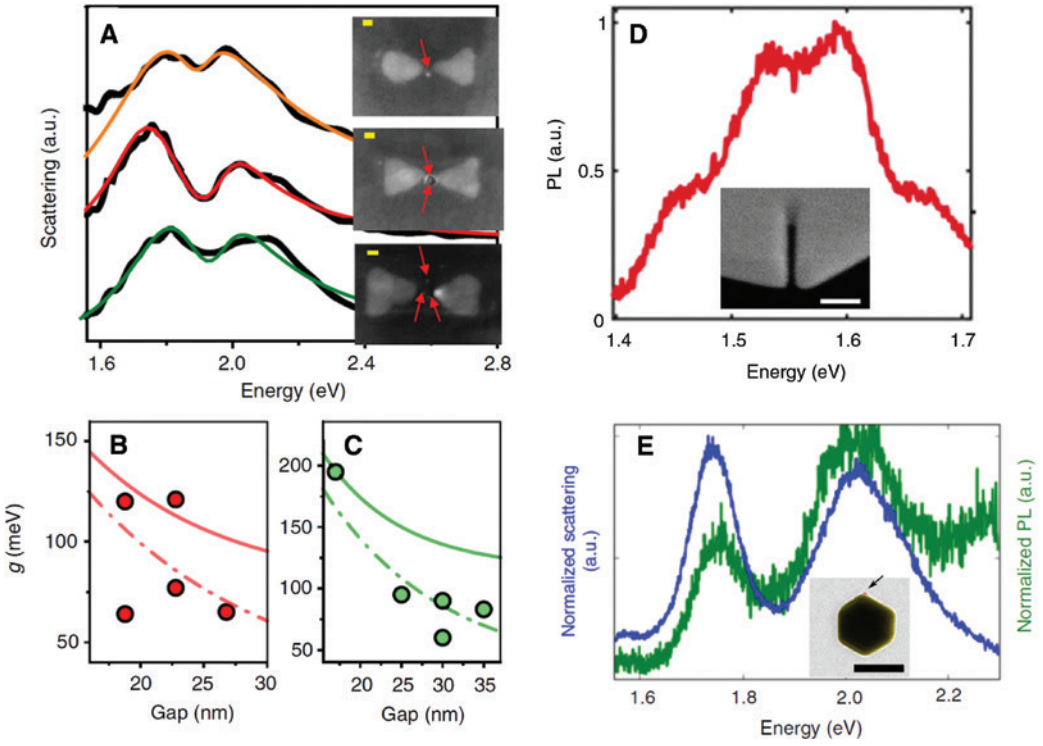

Figure 5: Observing strong coupling.
(A) Demonstration of the strong coupling between QDs and the plasmons of silver bowties. Scattering spectra of QD-PC hybrid systems along with their SEM images (scale bars, 20nm) show clear Rabi splitting. The red arrows point to the QDs in in the images. The colored lines are fits of the coupled oscillator model to the experimental data (black lines). (B, C) Dependence of coupling strengths on gap size for bowties with one QD (B) and two QDs (C). The continuous and dashed lines are numerically calculated coupling strengths with the QDs near one of the prisms (continuous lines) or with the QDs at the center of the bowtie (dashed-dotted lines). Panel (A), (B) and (C) are taken with permission from Santhosh et al. [139]. (D) PL spectra of a QD coupled to a plasmonic nanoresonator exhibiting a Rabi doublet due to the involvement of both neutral and charged excitions. Inset: SEM image of the nanoresonator fabricated at the apex of a scanning probe tip (scale bar, 100 nm). (E) Scattering spectra (blue) and PL spectra (green) of a plasmon-emitter system showing Rabi splitting. Inset: SEM images of the plasmon-emitter system. The QD is indicated by an arrow. Panels (D) & (E) are reprinted with permission from Groß et al. [140] and Leng et al. [141], respectively.

observed Rabi splitting was 288 meV. They also measured the variation of the coupling strength with increasing gap between the prisms of the bowties and showed that it compared favorably with numerical calculations (Figure 5B,C). This work has given momentum to studies involving single QDs. Indeed, Groß et al. [140] demonstrated strong coupling between a single QD and a plasmonic nanoresonator fabricated at the tip of a scanning probe (Figure 5D). This setup allowed precise control over the position of the cavity with respect to the QD, and hence tuning and optimization of the coupling strength. Four peaks were found in the emission spectra of the coupled QD-PC systems, and were attributed to coupling of both the neutral and charged excited states to the plasmons, with Rabi splitting values of 220 and 88 meV, respectively. The most recent contribution to studies of single QD coupling comes from Leng et al. [141]. These authors created a gap plasmon mode between a gold nanoparticle and a silver film, and positioned a QD there. A Rabi splitting as high as 230 meV was observed (Figure 5E). Clearly the strength of observed coupling with single QDs is increasing as fundamental understanding and device fabrication techniques are both improving.

7 Conclusion and outlook

Over the last years, novel experimental and theoretical studies of exciton-plasmon coupling involving QDs have resulted in deeper understanding of light-matter interactions at subwavelength scales. In this paper, we have attempted to provide a rather comprehensive review of these experimental and theoretical investigations along with a conceptual introduction to this exciting and growing field. Novel nanophotonic devices based on quantum plasmonics have been successfully designed to demonstrate weak and strong coupling between QDs and PCs. Figure 6 summarizes these achievements by positioning many of them on a continuous scale of coupling strength, g, starting from weak coupling and reaching strong coupling.

These experiments hold great potential for multiple future applications. Enhanced fluorescence intensity, a phenomenon which characterizes the weak coupling regime, is of merit in many applications involving fluorophores, such as sensing [36] and imaging [142], solar cells [143], light-emitting devices [144], lasers [145], single-photon

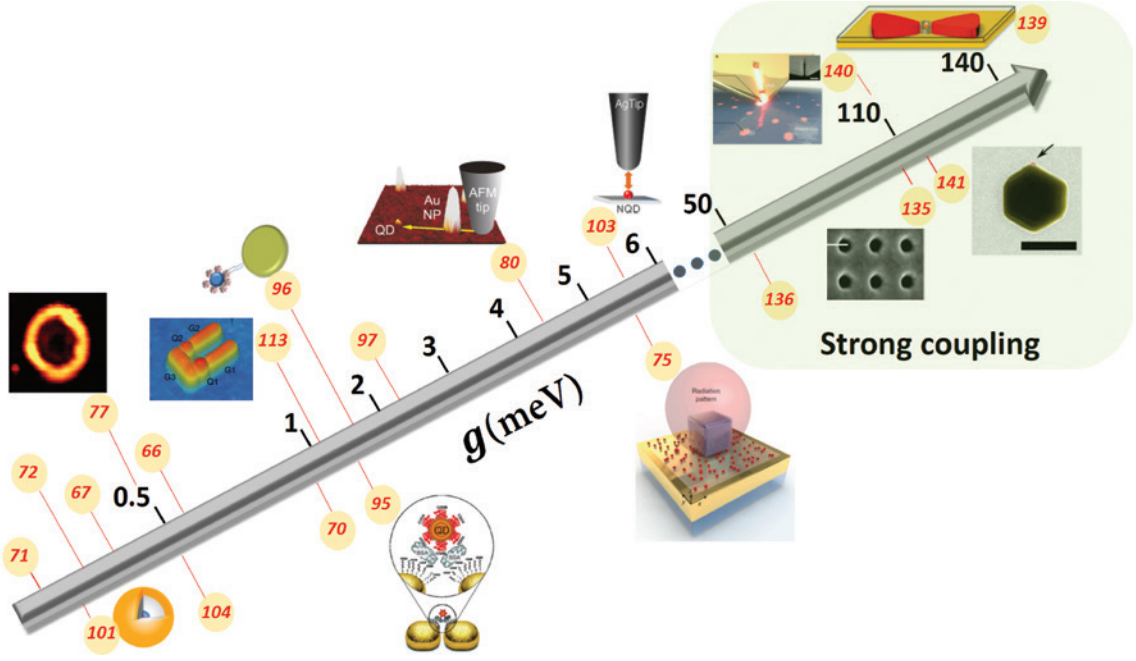

Figure 6: From weak to strong coupling.
Illustration of the range of coupling strengths, g, obtained from published work discussed in the review. The red numbers refer to the reference list. g values in the strong coupling regime were calculated as half of the Rabi splitting in observed spectra. The rest of the g values were calculated according to Hugall et al. [5]. Illustration figures are reprinted with permission from: Rakovich et al. [77] (copyright 2015), Ratchford et al. [80] (copyright 2011), Cohen-Hoshen [96] (copyright 2012) and Takata et al. [103] (copyright 2016), American Chemical Society. Ji et al. [101] is reprinted with permission from Springer Nature copyright 2015. Urena et al. [95] is reprinted from John Wiley and Sons, Advanced Materials, copyright 2012. Other figures are reprinted with permission from Hoang et al. [75], Tang et al. [113], Santhosh et al. [139], Groß et al. [140] and Leng et al. [141].

sources [146] and advanced optical communication devices [127]. One needs to understand the balance of the different contributions to the P signal and control light absorption and emission separately for optimal performance in the context of a specific application. For example, enhanced light absorption is the only desirable mechanism for thin-film solar cells [147] and photochemical reactions [148]. In contrast, in an electrically pumped organic light-emitting diode, maximizing the radiative decay rate is essential without regard to the absorption [149].

Multiple novel phenomena may also be demonstrated with QD-PC hybrid systems operating in the strong coupling regime. For example, light sources operating at the single photon level might be realized, and may not only be important from the fundamental quantum optics point of view but also in many advanced applications, such as quantum information processing [115], low threshold lasers [150] and more. Strong emitter-plasmon interactions will facilitate the realization of additional quantum optical devices such as optical switches at the single photon level [7].

Before concluding, we would like to discuss briefly a direction of research that is likely to be probed in the near future, and was so far only discussed theoretically [151–153], namely the quantum entanglement of two or more QDs within a PC. In the strong coupling regime, there is a periodic exchange of energy between the QD and the SP. If two spatially separated QDs are strongly coupled individually with the plasmons, it is possible that the two QDs will also be coupled, leading to quantum entanglement between them. Hensen et al. [151] used quantum dynamics calculations to demonstrate that two quantum emitters separated by more than 1.6 μm can be strongly coupled via a plasmon mode and quantum entanglement can be established on a short time scale of about 100 fs. Aeschlimann et al. [152] designed a plasmonic structure with two selectively addressable PCs position in the foci of an elliptical plasmonic resonator so that they are separated by ~twice their excitation wavelength. They demonstrated ultrafast long-range energy transfer between the two nanoatnennas and suggested that this scheme is suitable for coupling spatially separated quantum emitters positioned on them. It will be fascinating to observe experimentally the quantum entanglement between emitters using strong exciton-plasmon coupling in QD-PC devices.

References

[1] Novotny LA, Hecht B. Principles of nano-optics. New York, US, Cambridge University Press.
[2] Maier SA. Plasmonics: fundamentals and applications. New York, NY, US, Springer, 2007.
[3] Hernandez FE. Optics and plasmonics: fundamental studies and applications. Rev Plasmonics 2012:185–203.
[4] Novotny L, van Hulst N. Antennas for light. Nat Photon 2011;5:83–90.
[5] Hugall JT, Singh A, van Hulst NF. Plasmonic cavity coupling. ACS Photon 2018;5:43–53.
[6] Koenderink AF. Plasmon nanoparticle array waveguides for single photon and single plasmon sources. Nano Lett 2009;9:4228–33.
[7] Chang DE. Sørensen AS, Demler EA, Lukin MD. A single-photon transistor using nanoscale surface plasmons. Nat Phys 2007;3:807–12.
[8] Chen HMT, Zhao L, Wang F, Sun L-D, Wang J, Yan C-H, Plasmon-molecule interactions. Nano Today 2010;5:494–505.
[9] Chen H, Schatz GC, Ratner MA. Experimental and theoretical studies of plasmon-molecule interactions. Rep Prog Phys 2012;75:096402.
[10] Torma P, Barnes WL. Strong coupling between surface plasmon polaritons and emitters: a review. Rep Prog Phys 2015;78:013901.
[11] Willets AJ, Willets KA. Molecular plasmonics. Annu Rev Anal Chem 2016;9:27–45.
[12] Haran G, Chuntonov L. Artificial plasmonic molecules and their interaction with real molecules. Chem Rev 2018;118:5539–80.
[13] Rossetti R, Ellison JL, Gibson JM, Brus LE. Size effects in the excited electronic states of small colloidal CdS crystallites. J Chem Phys 1984;80:4464.
[14] Rosen AL, Rosen M. The electronic structure of semiconductor nanocrystals. Annu Rev Mater Sci. 2000;30:475–52.
[15] Gao X, Cui Y, Levenson RM, Chung LW, Nie S. In vivo cancer targeting and imaging with semiconductor quantum dots. Nat Biotechnol 2004;22:969–76.
[16] Jamieson T, Bakhshi R, Petrova D, Pocock R, Imani M, Seifalian AM. Biological applications of quantum dots. Biomaterials 2007;28:4717–32.
[17] Tian J, Cao G. Semiconductor quantum dot-sensitized solar cells. Nano Rev 2013;4:22578.
[18] Kairdolf BA, Smith AM, Stokes TH, Wang MD, Young AN, Nie S. Semiconductor quantum dots for bioimaging and biodiagnostic applications. Annu Rev Anal Chem 2013;6:143–62.
[19] Litvin AP, Martynenko IV, Purcell-Milton F, Baranov AV, Fedorov AV. Colloidal quantum dots for optoelectronics. J Mater Chem A 2017;5:13252.
[20] Ke Gong YZ, Kelley DF. Extinction coefficients, oscillator strengths, and radiative lifetimes of cdse, cdte, and cdte/cdse nanocrystals. J Phys Chem C 2013;117:20268–79.
[21] Xu S, Kumar S, Nann T. Rapid synthesis of high-quality InP nanocrystals. J Am Chem Soc 2006;128:1054–5.
[22] Fan J, Chu PK. Group IV nanoparticles: synthesis, properties, and biological applications. Small 2010;6:2080–98.
[23] Smyder JA, KraussTD. Coming attractions for semiconductor quantum dots. Mater Today 2011;14:382–7.
[24] Paul CLJ, Amalorpavam JP, Lee CW. Intraband optical transition energy in type-I group II to VI spherical quantum dots. J Nanophoton 2015;9:093069.
[25] Vasudevan D, Trinchi A, Gaddam RR, Cole I. Core–shell quantum dots: properties and applications. J Alloys Compounds 2015;636:395–404.

[26] Chan WC, Nie S. Quantum dot bioconjugates for ultrasensitive nonisotopic detection. Science 1998;281:2016–8.
[27] Dan Oron MK, Banin U. Multiexcitons in type-II colloidal semiconductor quantum dots. Phys Rev B 2007;75:035330.
[28] Sukhovatkin V, Hinds S, Brzozowski L, Sargent EH. Colloidal quantum-dot photodetectors exploiting multiexciton generation. Science 2009;324:1542–4.
[29] Reischle M, Beirne GJ, Rossbach R, Jetter M, Michler P. Influence of the dark exciton state on the optical and quantum optical properties of single quantum dots. Phys Rev Lett 2008;101:146402.
[30] Debasis Bera LQ, Tseng T-K, Holloway PH. Quantum dots and their multimodal applications: a review. Materials 2010;3:2260–45.
[31] Vahala KJ. Optical microcavities. Nature 2003;424:839–46.
[32] Haroche S, Raimond JM. Cavity Quantum Electrodynamics. Scientific American 1993;268:54–62.
[33] Zayats AV, Smolyaninov II, Maradudin AA. Nano-optics of surface plasmon polaritons. Phys Rep 2005;408:131–314.
[34] Barnes WL. Surface plasmon–polariton length scales: a route to sub-wavelength optics. J Opt A: Pure Appl Opt 2006;8:S87–93.
[35] Derrien TJY, Krüger J, Bonse J. Properties of surface plasmon polaritons on lossy materials: lifetimes, periods and excitation conditions. J Opt 2016;18:115007.
[36] Willets KA, Van Duyne RP. Localized surface plasmon resonance spectroscopy and sensing. Annu Rev Phys Chem 2007;58:267–97.
[37] Haes AJ, Haynes CL, Duyne RPV. Nanosphere lithography: self-assembled photonic and magnetic materials. Mat Res Soc Symp 2001;636.
[38] Link S, El-Sayed MA. Optical properties and ultrafast dynamics of metallic nanocrystals. Annu Rev Phys Chem 2003;54:331–66.
[39] Jean Lermé HB, Bonnet C, Broyer M, et al. Size dependence of the surface plasmon resonance damping in metal nanospheres. J Phys Chem Lett 2010;1:2922–8.
[40] Grigorchuk NI. Radiative damping of surface plasmon resonance in spheroidal metallic nanoparticle embedded in a dielectric medium. J Optical Soc Am B 2012;29:3404–11.
[41] Olson J, Dominguez-Medina S, Hoggard A, Wang LY, Chang WS, Link S. Optical characterization of single plasmonic nanoparticles. Chem Soc Rev 2015;44:40–57.
[42] Schlücker S. Surface-enhanced Raman spectroscopy: concepts and chemical applications. Angew Chem Int Ed Engl 2014;53:4756–95.
[43] Kurouski D, Lee H, Roschangar F, Senanayake C. Surface-enhanced Raman spectroscopy: from concept to practical application. Spectroscopy 2017;32.
[44] Aroca RF. Plasmon enhanced spectroscopy. Phys Chem Chem Phys 2013;15:5355–63.
[45] El-Sayed MA. Plasmonic photochemistry and photon confinement to the nanoscale. J Photochem Photobiol A: Chem 2011;221:138–42.
[46] Chu MW, Myroshnychenko V, Chen CH, Deng JP, Mou CY, Garcia de Abajo FJ. Probing bright and dark surface-plasmon modes in individual and coupled noble metal nanoparticles using an electron beam. Nano Lett 2009;9:399–404.
[47] Scholl JA, Koh AL, Dionne JA. Quantum plasmon resonances of individual metallic nanoparticles. Nature 2012;483:421–7.
[48] Esteban R, Vogelgesang R, Dorfmuller J, et al. Direct near-field optical imaging of higher order plasmonic resonances. Nano Lett 2008;8:3155–9.
[49] Halas NJ, Lal S, Chang WS, Link S, Nordlander P. Plasmons in strongly coupled metallic nanostructures. Chem Rev 2011;111:3913–61.
[50] Agarwal GS. Vacuum-field Rabi splittings in microwave absorption by Rydberg atoms in a cavity. Phys Rev Lett 1984;53:1732–4.
[51] Achermann M. Exciton-plasmon interactions in metal-semiconductor nanostructures. J Physl Chem Lett 2010;1:2837–43.
[52] Ming T, Chen HJ, Jiang RB, Li Q, Wang JF. Plasmon-controlled fluorescence: beyond the intensity enhancement. J Phys Chem Lett 2012;3:191–202.
[53] Yongqing Li QL, Zhang Z, Liu H, Lu X, Fang Y. Time-resolved photoluminescence spectroscopy of exciton-plasmon coupling dynamics. Plasmonics 2015;10:271–80.
[54] Park JE, Kim J, Nam JM. Emerging plasmonic nanostructures for controlling and enhancing photoluminescence. Chem Sci 2017;8:4696–704.
[55] Ruppin R. Decay of an excited molecule near a small metal sphere. J Chem Phys 1982;76:1681–4.
[56] Kuhn H. Classical aspects of energy transfer in molecular systems. J Chem Phys 1970;53:101–8.
[57] Moskovits M. Surface-enhanced spectroscopy. Rev Mod Phys 1985;57:783–826.
[58] Purcell EM. Spontaneous emission probabilities at radio frequencies. Phys Rev 1946;69.
[59] David A, Benisty H, Weisbuch C. Photonic crystal light-emitting sources. Rep Prog Phys 2012;75:126501.
[60] Forster T. Intermolecular energy transfer and fluorescence. Annalen der Physik 1948;2:55–75.
[61] Kosako T, Kadoya Y, Hofmann HF. Directional control of light by a nano-optical Yagi-Uda antenna. Nat Photon 2010;4:312–15.
[62] Curto AG, Volpe G, Taminiau TH, Kreuzer MP, Quidant R, van Hulst NF. Unidirectional emission of a quantum dot coupled to a nanoantenna. Science 2010;329:930–3.
[63] Kulakovich O, Strekal N, Yaroshevich A, et al. Enhanced luminescence of CdSe quantum dots on gold colloids. Nano Lett 2002;2:1449–52.
[64] Gryczynski I, Malicka J, Jiang W, et al. Surface-plasmon-coupled emission of quantum dots. J Phys Chem B 2005;109:1088–93.
[65] Koichi Okamoto SV, Scherer A. Surface-plasmon enhanced bright emission from CdSe quantum-dot nanocrystals. J Opt Soc Am B 2006;23:1674–8.
[66] Song JH, Atay T, Shi S, Urabe H, Nurmikko AV. Large enhancement of fluorescence efficiency from CdSe/ZnS quantum dots induced by resonant coupling to spatially controlled surface plasmons. Nano Lett 2005;5:1557–61.
[67] Brolo AG, Kwok SC, Cooper MD, et al. Surface plasmon-quantum dot coupling from arrays of nanoholes. J Phys Chem B 2006;110:8307–13.
[68] Ahmed SR, Cha HR, Park JY, Park EY, Lee D, Lee J. Photoluminescence enhancement of quantum dots on Ag nanoneedles. Nano Res Lett 2012;7:438.
[69] Chen YC, Munechika K, Jen-La Plante I, et al. Excitation enhancement of CdSe quantum dots by single metal nanoparticles. Appl Phys Lett 2008;93:053106.
[70] Wang Y, Yang T, Tuominen MT, Achermann M. Radiative rate enhancements in ensembles of hybrid metal-semiconductor nanostructures. Phys Rev Lett 2009;102:163001.
[71] Li X, Kao FJ, Chuang CC, He S. Enhancing fluorescence of quantum dots by silica-coated gold nanorods under one- and two-photon excitation. Opt Express 2010;18:11335–46.

[72] Munechika K, Chen Y, Tillack AF, et al. Quantum dot/plasmonic nanoparticle metachromophores with quantum yields that vary with excitation wavelength. Nano Lett 2011;11:2725–30.
[73] Belacel C, Habert B, Bigourdan F, et al. Controlling spontaneous emission with plasmonic optical patch antennas. Nano Lett 2013;13:1516–21.
[74] Nepal D, Drummy LF, Biswas S, Park K, Vaia RA. Large scale solution assembly of quantum dot-gold nanorod architectures with plasmon enhanced fluorescence. ACS Nano 2013;7:9064–74.
[75] Hoang TB, Akselrod GM, Argyropoulos C, Huang J, Smith DR, Mikkelsen MH. Ultrafast spontaneous emission source using plasmonic nanoantennas. Nat Commun 2015;6:7788.
[76] Guo R, Derom S, Vakevainen AI, et al. Controlling quantum dot emission by plasmonic nanoarrays. Opt Express 2015;23:28206–15.
[77] Rakovich A, Albella P, Maier SA. Plasmonic control of radiative properties of semiconductor quantum dots coupled to plasmonic ring cavities. ACS Nano 2015;9:2648–58.
[78] Ling Li WW, Luk TS, Yang X, Gao J. Enhanced quantum dot spontaneous emission with multilayer metamaterial nanostructures. 2017;4:501–8.
[79] Young Chul Jun RP, Mark L. Brongersma, Strong modification of quantum dot spontaneous emission via gap plasmon coupling in metal nanoslits. J Phys Chem C 2010;114:7269–73.
[80] Ratchford D, Shafiei F, Kim S, Gray SK, Li X. Manipulating coupling between a single semiconductor quantum dot and single gold nanoparticle. Nano Lett 2011;11:1049–54.
[81] Akimov AV, Mukherjee A, Yu CL, et al. Generation of single optical plasmons in metallic nanowires coupled to quantum dots. Nature 2007;450:402–6.
[82] Lassiter JB, McGuire F, Mock JJ, et al. Plasmonic waveguide modes of film-coupled metallic nanocubes. Nano Lett 2013;13:5866–72.
[83] Akselrod GM, Argyropoulos C, Hoang TB, et al. Probing the mechanisms of large Purcell enhancement in plasmonic nanoantennas. Nat Photon 2014;8:835–40.
[84] Busson MP, Rolly B, Stout B, Bonod N, Bidault S. Accelerated single photon emission from dye molecule-driven nanoantennas assembled on DNA. Nat Commun 2012;3:962.
[85] Russell KJ, Liu T-L, Cui S, Hu EL. Large spontaneous emission enhancement in plasmonic nanocavities. Nat Photon 2012;6:459–62.
[86] Punj D, Mivelle M, Moparthi SB, et al. A plasmonic 'antenna-in-box' platform for enhanced single-molecule analysis at micromolar concentrations. Nat Nanotechnol 2013;8:512–6.
[87] Khatua S, Paulo PM, Yuan H, Gupta A, Zijlstra P, Orrit M. Resonant plasmonic enhancement of single-molecule fluorescence by individual gold nanorods. ACS Nano 2014;8:4440–9.
[88] Abadeer NS, Brennan MR, Wilson WL, Murphy CJ. Distance and plasmon wavelength dependent fluorescence of molecules bound to silica-coated gold nanorods. ACS Nano 2014;8:8392–406.
[89] Benz F, Schmidt MK, Dreismann A, et al. Single-molecule optomechanics in "picocavities". Science 2016;354:726–9.
[90] Shimizu KT, Woo WK, Fisher BR, Eisler HJ, Bawendi MG. Surface-enhanced emission from single semiconductor nanocrystals. Phys Rev Lett 2002;89:117401.
[91] Farahani JN, Pohl DW, Eisler HJ, Hecht B. Single quantum dot coupled to a scanning optical antenna: a tunable superemitter. Phys Rev Lett 2005;95:017402.
[92] Yuichi Ito KM, Kanemitsu Y. Mechanism of photoluminescence enhancement in single semiconductor nanocrystals on metal surfaces. Phys Rev B 2007;75:033309.
[93] Xuedan Ma HT, Kipp T, Mews A. Fluorescence enhancement, blinking suppression, and gray states of individual semiconductor nanocrystals close to gold nanoparticles. Nano Lett 2010;10:4166–74.
[94] Shafran E, Mangum BD, Gerton JM. Using the near-field coupling of a sharp tip to tune fluorescence-emission fluctuations during quantum-dot blinking. Phys Rev Lett 2011;107:037403.
[95] Urena EB, Kreuzer MP, Itzhakov S, et al. Excitation enhancement of a quantum dot coupled to a plasmonic antenna. Adv Mater 2012;24:OP314–20.
[96] Cohen-Hoshen E, Bryant GW, Pinkas I, Sperling J, Bar-Joseph I. Exciton-plasmon interactions in quantum dot-gold nanoparticle structures. Nano Lett 2012;12:4260–4.
[97] Yuan CT, Wang YC, Cheng HW, et al. Modification of fluorescence properties in single colloidal quantum dots by coupling to plasmonic gap modes. J Phys Chem C 2013;117:12762–8.
[98] Gruber C, Trugler A, Hohenau A, Hohenester U, Krenn JR. Spectral modifications and polarization dependent coupling in tailored assemblies of quantum dots and plasmonic nanowires. Nano Lett 2013;13:4257–62.
[99] Sharonda J, LeBlanc MRM, Jones M, Moyer PJ. Enhancement of Multiphoton emission from single CdSe quantum dots coupled to gold films. Nano Lett. 2013;13:1662–9.
[100] Meixner AJ, Jager R, Jager S, et al. Coupling single quantum dots to plasmonic nanocones: optical properties. Faraday Discuss 2015;184:321–37.
[101] Ji B, Giovanelli E, Habert B, et al. Non-blinking quantum dot with a plasmonic nanoshell resonator. Nat Nanotechnol 2015;10:170–5.
[102] Thomas Hartsfield MG, Su P-H, Buck MR, et al. Semiconductor quantum dot lifetime near an atomically smooth Ag film exhibits a narrow distribution. ACS Photon 2016;3:1085–9.
[103] Takata H, Naiki H, Wang L, et al. Detailed observation of multiphoton emission enhancement from a single colloidal quantum dot using a silver-coated AFM tip. Nano Lett 2016;16:5770–8.
[104] Matsuzaki K, Vassant S, Liu HW, et al. Strong plasmonic enhancement of biexciton emission: controlled coupling of a single quantum dot to a gold nanocone antenna. Sci Rep 2017;7:42307.
[105] Li Q, Wei H, Xu H. Resolving single plasmons generated by multiquantum-emitters on a silver nanowire. Nano Lett 2014;14:3358–63.
[106] Li Q, Wei H, Xu H. Quantum yield of single surface plasmons generated by a quantum dot coupled with a silver nanowire. Nano Lett 2015;15:8181–7.
[107] Yurui Fang HW, Hao F, Nordlander P, Xu H. Remote-excitation surface-enhanced raman scattering using propagating Ag nanowire plasmons. Nano Lett 2009;9:2049–53.
[108] Yingzhou Huang YF, Zhang Z, Zhu L, Sun M. Nanowire-supported plasmonic waveguide for remote excitation of surface-enhanced Raman scattering. Light: Sci Appl 2014;3:199.
[109] de Torres J, Ferrand P, Colas des Francs G, Wenger J. Coupling emitters and silver nanowires to achieve long-range plasmon-mediated fluorescence energy transfer. ACS Nano 2016;10:3968–76.

[110] Aouani H, Mahboub O, Bonod N, et al. Bright unidirectional fluorescence emission of molecules in a nanoaperture with plasmonic corrugations. Nano Lett 2011;11:637–44.
[111] Aouani H, Mahboub O, Devaux E, Rigneault H, Ebbesen TW, Wenger J. Plasmonic antennas for directional sorting of fluorescence emission. Nano Lett 2011;11:2400–6.
[112] Cao SH, Cai WP, Liu Q, Li YQ. Surface plasmon-coupled emission: what can directional fluorescence bring to the analytical sciences? Annu Rev Anal Chem 2012;5:317–36.
[113] Tang J, Xia J, Fang M, et al. Selective far-field addressing of coupled quantum dots in a plasmonic nanocavity. Nat Commun 2018;9:1705.
[114] Yoshie T, Scherer A, Hendrickson J, et al. Vacuum Rabi splitting with a single quantum dot in a photonic crystal nanocavity. Nature 2004;432:200–3.
[115] Reithmaier JP, Sek G, Loffler A, et al. Strong coupling in a single quantum dot-semiconductor microcavity system. Nature 2004;432:197–200.
[116] Peter E, Senellart P, Martrou D, et al. Exciton-photon strong-coupling regime for a single quantum dot embedded in a microcavity. Phys Rev Lett 2005;95:067401.
[117] Hobson PA, Barnes WL, Lidzey DG, et al. Strong exciton-photon coupling in a low-Q all-metal mirror microcavity. Appl Phys Lett 2002;81:3519–21.
[118] Coles DM, Somaschi N, Michetti P, et al. Polariton-mediated energy transfer between organic dyes in a strongly coupled optical microcavity. Nat Mater 2014;13:712–9.
[119] Daskalakis KS, Maier SA, Murray R, Kena-Cohen S. Nonlinear interactions in an organic polariton condensate. Nat Mater 2014;13:271–8.
[120] Liu XZ, Galfsky T, Sun Z, et al. Strong light-matter coupling in two-dimensional atomic crystals. Nat Photon 2015;9:30–34.
[121] Dintinger J, Klein S, Bustos F, Barnes WL, Ebbesen TW. Strong coupling between surface plasmon-polaritons and organic molecules in subwavelength hole arrays. Phys Rev B 2005;71:035424.
[122] Fofang NT, Park TH, Neumann O, Mirin NA, Nordlander P, Halas NJ. Plexcitonic nanoparticles: plasmon-exciton coupling in nanoshell-j-aggregate complexes. Nano Lett 2008;8:3481–7.
[123] Vasa P, Wang W, Pomraenke R, et al. Real-time observation of ultrafast Rabi oscillations between excitons and plasmons in metal nanostructures with J-aggregates. Nat Photon 2013;7:128–32.
[124] Chikkaraddy R, de Nijs B, Benz F, et al. Single-molecule strong coupling at room temperature in plasmonic nanocavities. Nature 2016;535:127–30.
[125] Wersall M, Cuadra J, Antosiewicz TJ, et al. Observation of mode splitting in photoluminescence of individual plasmonic nanoparticles strongly coupled to molecular excitons. Nano Lett 2017;17:551–8.
[126] Bellessa J, Bonnand C, Plenet JC, Mugnier J. Strong coupling between surface plasmons and excitons in an organic semiconductor. Phys Rev Lett 2004;93:036404.
[127] Chang DE, Sorensen AS, Hemmer PR, Lukin MD. Quantum optics with surface plasmons. Phys Rev Lett 2006;97:053002.
[128] Trügler A, Hohenester U. Strong coupling between a metallic nanoparticle and a single molecule. Phys Rev B – Condensed Matter and Materials Physics 2008;77:115403.
[129] Savasta S, Saija R, Ridolfo A, Di Stefano O, Denti P, Borghese F. Nanopolaritons: vacuum rabi splitting with a single quantum dot in the center of a dimer nanoantenna. ACS Nano 2010;4:6369–76.
[130] D'Agostino S, Alpeggiani F, Andreani LC. Strong coupling between a dipole emitter and localized plasmons: enhancement by sharp silver tips. Opt Express 2013;21:27602.
[131] Gómez DE, Giessen H, Davis TJ. Semiclassical plexcitonics: simple approach for designing plexcitonic nanostructures. J Phys Chem C 2014;118:23963–9.
[132] Słowik K, Filter R, Straubel J, Lederer F, Rockstuhl C. Strong coupling of optical nanoantennas and atomic systems. Phys Rev B - Condensed Matter Materials Physics 2013;88:1–12.
[133] Haroche S, Raimond J-M. Exploring the quantum: atoms, cavities, and photons. Oxford University Press: Oxford, 2013.
[134] Jaynes ET, Cummings FW. Comparison of quantum and semiclassical radiation theories with application to the beam maser. Proc IEEE 1963;51:89–109.
[135] Wang H, Wang H-Y, Toma A, et al. Dynamics of strong coupling between CdSe quantum dots and surface plasmon polaritons in subwavelength hole array. J Phys Chem Lett 2016;7:4648–54.
[136] Gomez DE, Vernon KC, Mulvaney P, Davis TJ. Surface plasmon mediated strong exciton- photon coupling in semiconductor nanocrystals. Nano Lett 2009;10:274–8.
[137] Gómez DE, Vernon KC, Mulvaney P, Davis TJ. Coherent superposition of exciton states in quantum dots induced by surface plasmons. Appl Phys Lett 2010;96:073108.
[138] Gomez DE, Lo SS, Davis TJ, Hartland GV. Picosecond kinetics of strongly coupled excitons and surface plasmon polaritons. J Phys Chem B 2013;117:4340–6.
[139] Santhosh K, Bitton O, Chuntonov L, Haran G. Vacuum Rabi splitting in a plasmonic cavity at the single quantum emitter limit. Nat Comm 2016;7:ncomms11823.
[140] Groß H, Hamm JM, Tufarelli T, Hess O, Hecht B. Near-field strong coupling of single quantum dots. Sci Adv 2018;4:eaar4906.
[141] Leng H, Szychowski B, Daniel MC, Pelton M. Strong coupling and induced transparency at room temperature with single quantum dots and gap plasmons. Nat Commun 2018;9:4012.
[142] Ropp C, Cummins Z, Nah S, Fourkas JT, Shapiro B, Waks E. Nanoscale imaging and spontaneous emission control with a single nano-positioned quantum dot. Nat Commun 2013;4:1447.
[143] Brown MD, Suteewong T, Kumar RS, et al. Plasmonic dye-sensitized solar cells using core-shell metal-insulator nanoparticles. Nano Lett 2011;11:438–45.
[144] Lozano G, Rodriguez SR, Verschuuren MA, Gomez Rivas J. Metallic nanostructures for efficient LED lighting. Light Sci Appl 2016;5:e16080.
[145] Gupta S, Waks E. Overcoming Auger recombination in nanocrystal quantum dot laser using spontaneous emission enhancement. Opt Express 2014;22:3013–27.
[146] Gazzano O, Michaelis de Vasconcellos S, Gauthron K, et al. Single photon source using confined Tamm plasmon modes. Appl Phys Lett 2012;100:232111.
[147] Yang Z, Fan JZ, Proppe AH, et al. Mixed-quantum-dot solar cells. Nat Commun 2017;8:1325.
[148] Robatjazi H, Zhao H, Swearer DF, et al. Plasmon-induced selective carbon dioxide conversion on earth-abundant aluminum-cuprous oxide antenna-reactor nanoparticles. Nat Commun 2017;8:27.

[149] Gu X, Qiu T, Zhang W, Chu PK. Light-emitting diodes enhanced by localized surface plasmon resonance. Nanoscale Res Lett 2011;6:199.
[150] Noda S. Applied physics. Seeking the ultimate nanolaser. Science 2006;314:260–1.
[151] Hensen M, Heilpern T, Gray SK, Pfeiffer W. Strong coupling and entanglement of quantum emitters embedded in a nanoantenna-enhanced plasmonic cavity. ACS Photon 2017;5:240–8.
[152] Aeschlimann M, Brixner T, Cinchetti M, et al. Cavity-assisted ultrafast long-range periodic energy transfer between plasmonic nanoantennas. Light: Sci Appl 2017;6:e17111.
[153] Otten M, Larson J, Min MS, Wild SM, Pelton M, Gray SK. Origins and optimization of entanglement in plasmonically coupled quantum dots. Phys Rev A 2016;94:022312.